Title

Reciprocal activation of HEY1 and NOTCH4 under SOX2 control promotes EMT in head and neck squamous cell carcinoma

Journal

International Journal of Oncology, 58(2)

ISSN

1019-6439

Authors

Fukusumi, Takahito
Guo, Theresa W
Ren, Shuling
et al.

Publication Date

2021-02-01

DOI

10.3892/ijo.2020.5156

Peer reviewed

Reciprocal activation of *HEY1* and *NOTCH4* under *SOX2* control promotes EMT in head and neck squamous cell carcinoma

TAKAHITO FUKUSUMI[1,2], THERESA W. GUO[1,3], SHULING REN[1], SUNNY HAFT[1], CHAO LIU[1], AKIHIRO SAKAI[4], MIZUO ANDO[5], YUKI SAITO[5], SAYED SADAT[1] and JOSEPH A. CALIFANO[1,3]

[1]Moores Cancer Center, University of California, San Diego, La Jolla, CA 92093, USA; [2]Department of Otorhinolaryngology-Head and Neck Surgery, Osaka University Graduate School of Medicine, Suita, Osaka 565-0871, Japan; [3]Division of Otolaryngology-Head and Neck Surgery, Department of Surgery, University of California, San Diego, La Jolla, CA 92093, USA; [4]Department of Otolaryngology-Head and Neck Surgery, Tokai University, School of Medicine, Isehara, Kanagawa 259-1193; [5]Department of Otolaryngology-Head and Neck Surgery, University of Tokyo, Tokyo 113-8655, Japan

Received November 9, 2019; Accepted October 8, 2020

DOI: 10.3892/ijo.2020.5156

Abstract. Several comprehensive studies have demonstrated that the *NOTCH* pathway is altered in a bimodal manner in head and neck squamous cell carcinoma (HNSCC). In a previous study, it was found that the *NOTCH4*/*HEY1* pathway was specifically upregulated in HNSCC and promoted epithelial-mesenchymal transition (EMT), and that *HEY1* activation supported *SOX2* expression. However, the interactions in this pathway have not yet been fully elucidated. The present study investigated the *NOTCH4*/*HEY1*/*SOX2* axis in HNSCC using *in vitro* models and the Cancer Genome Atlas (TCGA) database. To explore the association, reporter and ChIP RT-qPCR assays using *SOX2*-overexpressing (*SOX2*-OE) cells were performed. The association between *NOTCH4* and *HEY1* was examined in the same manner using *HEY1*-overexpressing (*HEY1*-OE) cells. The results of the *in vitro* experiments indicated that *HEY1* promoted EMT in the HNSCC cells. Furthermore, the overexpression of *HEY1* also promoted sphere formation and increased murine xenograft tumorigenicity. Reporter assays and ChIP RT-qPCR experiments indicated that *SOX2* regulated *HEY1* expression via direct binding of the *HEY1* promoter. *HEY1* expression significantly correlated with *SOX2* expression in primary lung SCC and other SCCs using the TCGA database. *HEY1* also regulated *NOTCH4* expression to create a positive reciprocal feedback loop. On the whole, the present study demonstrates that *HEY1* expression in HNSCC is regulated via the promotion of *SOX2* and promotes EMT. The *NOTCH4*/*HEY1* pathway is specifically upregulated via a positive reciprocal feedback loop mediated by the *HEY1*-medaited regulation of *NOTCH4* transcription, and *SOX2* correlates with *HEY1* expression in SCC from other primary sites.

Correspondence to: Professor Joseph A. Califano, Division of Otolaryngology-Head and Neck Surgery, Department of Surgery, University of California, 9500 Gilman Drive, San Diego, La Jolla, CA 92093, USA
E-mail: jcalifano@ucsd.edu

Key words: head and neck squamous cell carcinoma, TCGA, *SOX2*, *NOTCH4*, *HEY1*

Introduction

Head and neck squamous cell carcinoma (HNSCC) is the sixth most common malignancy, with >600,000 cases diagnosed annually worldwide (1). Half of the patients with HNSCC are diagnosed in an advanced stage at the first medical examination. In addition, >50% of recurrences occur within 3 years following treatment (2-4). Similar to other types of cancer, the accumulation of genetic and epigenetic alternations is considered to generate and promote HNSCC. Recently, several comprehensive analyses for HNSCC gene mutations were performed using high-throughput next generation sequencing defining *NOTCH1* mutation at a 10-15% rate. This rate is the second most frequent following *TP53* and higher than previously considered (5,6). Subsequently a previous study demonstrated a bimodal pattern of *NOTCH* pathway alterations in HNSCC, with a smaller subset of HNSCC exhibiting inactivating *NOTCH1* receptor mutations, but a larger subset exhibiting *NOTCH* pathway activating alterations, resulting in downstream *HES1*/*HEY1* pathway activation (7).

HES, HEY, CCND1, MYC, BCL-2 and *p21* are *NOTCH* target genes. Among these genes, the *HES* and *HEY* families are considered prominent downstream effectors of the *NOTCH* pathway (8,9). *HEY1* is known to promote epithelial-mesenchymal transition (EMT) in several normal tissues, such as the epidermis, kidney tubules, mammary gland and endocardia (10-12). *HEY1* knockdown in glioblastoma cells has been shown to decrease colony formation and invasion (13). A previous study demonstrated that *HEY1* expression in a skin human SCC cell line was increased under 3D culture and promoted an EMT phenotype (14). Man *et al* indicated that HNSCC exhibits a significantly higher *HEY1* expression than

normal epithelial cells (15). Recently, *HEY1* has been shown to be associated with a poor prognosis, independent of *NOTCH1* expression, indicating that other *NOTCH* members may drive *HEY1* expression as a key pathway alteration in HNSCC (16). In a previous study, it was also found that the *NOTCH4*/*HEY1* pathway was specifically upregulated in HNSCC and it was revealed that this pathway promoted EMT (17). However, the mechanisms that effect *NOTCH4*/*HEY1* pathway activation in HNSCC remain unclear.

SOX2, as well as *CD10* (18), *CD44* (19) and *ALDH1* (20) are HNSCC cancer stem cell (CSC) markers (21). *SOX2* expression in HNSCC is significantly related to a worse prognosis (22) and *SOX2* promotes migration, invasion and EMT in HNSCC (23). To define *NOTCH* downstream effectors, the present study examined the association between *SOX2* and *HEY1*. The authors previously demonstrated that *HEY1* knockdown significantly decreased *NOTCH4* expression and decreased *SOX2* expression in HNSCC cells (17). To further define these associations, the present study examined specific feedback loops between *HEY1* and *NOTCH4* and *SOX2* in HNSCC.

Materials and methods

Cells and cell culture. Cal27, SCC61 and SCC090 HNSCC cell lines were used in the present study. Cal27 and SCC090 cells were obtained from the Gutkind Laboratory at the University of California San Diego, Moores Cancer Center. SCC61 cells were obtained from the Weichselbaum Laboratory at the University of Chicago. SCC090 cells were originally established from human papilloma virus (HPV)-positive HNSCC tissues. The other two cells were established from HPV-negative HNSCC tissues. These cells were cultured in Dulbecco's modified Eagle's medium (DMEM; Sigma-Aldrich; Merck KGaA) supplemented with 10% fetal bovine serum (FBS) and a penicillin (50 U/ml) and streptomycin (50 μg/ml) cocktail. All cells were cultured under an atmosphere of 5% CO_2 at 37˚C.

Vector transfection. A lenti-ORF clone of human *SOX2* (#RC200757L3), *HEY1* (#RC200257L3) and an empty vector control (#PS100092) were obtained from OriGene Technologies, Inc. The 293T cells obtained from the Gutkind Laboratory were seeded in 6-well plates one day prior to transfection, and each construct was transfected in Opti-MEM (#31985070, Thermo Fisher Scientific, Inc.) and Turbofect transfection reagent (#R0531, Thermo Fisher Scientific, Inc.). Viral supernatants were consisted of 10 μg lentiviral plasmid, 6.67 μg packaging vector and 3.33 μg envelope per well in 6 well plates, and collected at 48 and 72 h following transfection. Cal27, SCC61 and SCC090 cells were seeded one day prior to infection in a 6-well plate and allowed to reach 50-60% confluency. The virus supernatant and 2 μl of polybrene (Sigma-Aldrich; Merck KGaA) were added to the cells. Cells were maintained under puromycin (#ant-pr-1, Invivogen; Thermo Fisher Scientific, Inc.) selection at a 1-μg/ml concentration. The following experiments using *SOX2* and *HEY1* overexpression cells were compared empty vector control transfected cells in Cal27, SCC61 and SCC090.

Reverse transcription-quantitative PCR (RT-qPCR). To validate mRNA expression levels in each experiment, RT-qPCR was used. Briefly, total RNA was extracted from the cells using the RNeasy plus mini kit (Qiagen GmbH), and complementary DNA was synthesized using a high-capacity cDNA reverse transcription kit (Thermo Fisher Scientific, Inc.). All primers were obtained from TaqMan Gene Expression assays (cat. no. 4331182. Thermo Fisher Scientific, Inc.). Each gene ID is described as follows: *β-actin (ACTB)*: Hs01060665_g1; *NOTCH4*: Hs00965895_g1; *HES1*: Hs00172878_m1; *HEY1*: Hs01114113_m1; *E-cadherin*: Hs01023895_m1; *fibronectin*: Hs01549976_m1; *Vimentin*: Hs00958111_m1; *TWIST1*: Hs01675818_s1; and *SOX2*: Hs01053049_s1. The thermocycle program was set at 95˚C for 10 min, followed by 50 cycles of denaturation at 95˚C for 15 sec and annealing at 60˚C for 60 sec. PCR quantification was conducted using the ΔΔCq method (24). qPCR was performed using the Quant Studio 6 Flex Real-Time PCR System (Thermo Fisher Scientific, Inc.).

Western blot analysis. Protein was obtained from the Cal27, SCC61 and SCC090 cells, and lysed with RIPA buffer (50 mm Tris-HCl pH 8.0, 150 mm NaCl, 1% IGE-PAL CA 630, 0.5% Na-DOC, and 0.1% SDS). Total protein concentrations were measured using Bio-Rad protein assay kit (Bio-Rad Laboratories, Inc.). 10 μl Equal amount of protein was set on Mini-PROTEAN TGX gels (Bio-Rad Laboratories, Inc.). The following primary antibodies were added to nitrocellulose membranes with 5% non-fat dry milk in Tris-buffered saline and 1% Tween-20, and incubated at 4˚C overnight: NOTCH4 (1:500, #2423, Cell Signaling Technology, Inc.), HES1 (1:1,000, #sc-25392, Santa Cruz Biotechnology, Inc.), HEY1 (1:400, #ab22614, Abcam), E-cadherin (1:10,000, #610181, BD Biosciences), fibronectin (1:3,000, #ab2413, Abcam), Vimentin (1:500, #V6630, Sigma-Aldrich; Merck KGaA), TWIST1 (1:1,000, #sc-15393, Santa Cruz Biotechnology, Inc.) and SOX2 (1:1,000, #2748, Cell Signaling Technology, Inc.). HRP-conjugated goat anti-mouse (#1010-05, 1:20,000 dilution; SouthernBiotech) or anti-rabbit antibodies (#4010-05, 1:20,000 dilution; SouthernBiotech) were used as secondary antibodies. These secondary antibodies were incubated at room temperature for 1 h. Western blots were developed using Pierce ECL Western Blotting Substate (Thermo Fisher Scientific).

Migration and invasion assays. Migration assays were performed in cell culture inserts (24-well, 8-μm pore size, #353097, Corning, Inc.). Cell concentrations ranged from 10^5 to $2x10^5$ cells/ml. Invasion assays were also performed in Corning BioCoat Matrigel invasion chambers (24-well, 8-μm pore size, #353097, Corning, Inc.). Cell concentrations ranged from $2x10^5$ to $4x10^5$ cells/ml. Cells were seeded on uncoated or Matrigel-coated inserts in 500 ml of serum-free medium for migration and invasion assays, respectively. The lower chambers were filled with 750 μl of 10% FBS-supplemented medium. After 48 h, the cells on the lower surface of the insert were fixed and stained with crystal violet (Differential Quik Stain kit, Polysciences) at room temperature for 2 min. The number of stained cells was counted in >3 fields under an inverted microscope (Olympus CKX31).

Sphere formation assay. Cells were seeded in 96-well ultralow attachment culture dishes (Corning, Inc.) at 10-100 cells/well.

Media consisted of serum-free DMEM/F12 Glutamax supplement medium (#10565042, Thermo Fisher Scientific, Inc.), basic fibroblast growth factor (bFGF: 20 ng/ml, #13256029, Thermo Fisher Scientific, Inc.), epithelial growth factor (EGF: 20 ng/ml, #PHG0313, Thermo Fisher Scientific, Inc.), B-27 (1:50 dilution, #17504044, Thermo Fisher Scientific, Inc.) and N2 supplement (1:100 dilution, #17502-048, Thermo Fisher Scientific, Inc.). Images were obtained at 10 days after seeding using a clinical upright microscope (Olympus, BX43) (Fig. 2A), and the numbers of sphere colonies in each well were counted using an inverted microscope (Olympus CKX31).

Cell viability assay. Cells were seeded in 96-well plates at 1,500 to 9,000 cells/well. Cell numbers were measured on day 3. Cell viabilities were measured using Vita Blue Cell Viability reagent (Bimake.com). Following a 1.5-h pre-incubation at 37˚C in the assay solution, the viable cell number in each well was calculated using fluorescence (Ex=530-570 nm, Em=590-620 nm) in a microplate reader (BioTek Insturments, Inc.). The assays were performed ≥3 times.

Mouse xenograft models. Cells ($2x10^6$) were diluted in 200 ml and injected subcutaneously into nude mice (Charles River Laboratories, Inc.) using a 25-gauge needle. Mice were anesthetized with a mixture of oxygen and isoflurane (5% in air for induction and 2% for maintenance) prior to each experiment, such as cell injection and tumor size measurement. Mice were maintained under pathogen-free conditions and sacrificed 2 months later or when tumors exceeded 20 mm at the largest diameter or earlier if necessary [this was done if any animal was observed to be cachexic (weight loss >15% from starting weight), moribund, dehydrated, anorexic, or any tumor that was ulcerated or eroded]. Mice were euthanized using carbon dioxide gas for 10 min. The CO_2 flow rate displaced 15-25% of the camber volume. Mice were euthanized in November, 2017. The confirmation of euthanasia was assured by verifying the absence of respiration, cardiac function and toe/tail pinch reflexes at least 10 min. Mice were handled in accordance with the procedures outlined in the Regulations on Animal Experiments at University of California San Diego. The Institutional Animal Care and Use Committee at the University of California San Diego approved the study.

Immunohistochemistry. Mouse xenograft tumors were stained overnight at 4˚C with a *HEY1* primary antibody (#ab22614, Abcam) diluted 1:100 in PBS with 2.5% BSA. Biotinylated IgG antibody (#BA-1000, Vector Laboratories, Inc.) were used at 1:400 as a secondary antibody for 30 min at room temperature. Staining was developed at room temperature for 2 min with DAB. Specimens were counterstained at room temperature for 1 min with hematoxylin and mounted with glycerol gelatin. A clinical upright microscope (Olympus, BX439) was used to examine these specimens.

TCGA dataset. The mRNA expression sequence data of patients with HNSCC were obtained from the firebrowse website (http://firebrowse.org/). These TCGA data included 522 HNSCC and 44 normal tissues. In total, 447 HNSCC cases were used for *NOTCH* analysis, excluding 73 tumors with *NOTCH* mutations. RNA expression was normalized by RSEM.

Reporter assay. Promoter reporter clone for human *NOTCH4* (#HPRM45581-LvPG04), *HEY1* (#HPRM10038-LvPG04) and negative control (#NEG-LvPG04) containing a 1,443 bp region of the *NOTCH4* promoter regions and the *HEY1* reporter assay based on a 1,455 bp region of the *HEY1* promoter region, respectively, were obtained from GeneCopoeia, Inc. The Cal27, SCC61 and SCC090 cells were transfected using 2.0 μg of these clones and 6 μl of X-tremeGENE 9 (Roche) per well in 6 well plates, and incubated at 37˚C for 24 h. The culture medium was collected 48 h after transfection. The Secrete-Pair Dual Luminescence Assay kit (#LF032, GeneCopoeia, Inc.) was used that was optimized using these promoter reporter clones to validate each promoter activity and the promoter activities were examined using the manufacturer's protocol.

Chromatin immunoprecipitation qPCR. For chromatin immunoprecipitation (ChIP) qPCR assays, the SimpleChIP Plus Enzymatic Chromatin IP kit (#9005, Cell Signaling Technology, Inc.) was used. Chromatin was incubated overnight with antibodies for *SOX2* (#2748, Cell Signaling Technology, Inc.) or *HEY1* (#19929-1-AP, ProteinTech Group, Inc.) at 4˚C under rotation. Chromatin was incubated with a polyclonal rabbit IgG as a negative control and Histone H3 (D2B12) XP-Rabbit mAb as positive control that were included in the ChIP kit. Primer sequences for qPCR were obtained from Integrated DNA Technologies, Inc. The following primer sequences were used: *HEY1* promoter forward, 5'-CCCGCTGAGAGGATCTG-3' and reverse, 5'-CCCTGTGCATCTCATTTCC-3'; *NOTCH4* promoter forward, 5'-AGTGGTGCTGGTGAAGTA-3' and reverse, 5'-CCACACACTGAGTTCCTTTAG-3'. The results were computed as percentage antibody bound per input DNA and normalized to the IgG controls using the Quant Studio 6 Flex Real-Time PCR System (Thermo Fisher Scientific, Inc.).

Statistical analysis. All *in vitro* experiments were performed at least in triplicate. Statistical comparisons of 2 groups were determined using the Student's t-test. For the comparisons of multiple group against the control group, Dunnett's test was used. The correlation between the expression of 2 genes was determined with Pearson's correlation analysis. Differences were considered significant at $P<0.05$. All statistical analyses were performed using JMP 12 software (SAS, Inc.).

Results

HEY1 promotes HNSCC EMT, migration and invasion. Previously, the authors demonstrated that *HEY1* promoted EMT in HNSCC cells using cells in which *HEY1* was knocked down (17). To validate this finding, the present study generated stable *HEY1*-overexpressing (*HEY1*-OE) and control cells using the Cal27, SCC61 and SCC090 cell lines (Figs. 1A and S1A). The results of RT-qPCR revealed that mesenchymal gene expression (*fibronectin, Vimentin* and *TWIST1*) in the *HEY1*-OE cells significantly increased in all HNSCC cells. However, *E-cadherin* expression was higher in the Cal27 *HEY1*-OE than in the control cells, with no significant differences observed between the SCC61 and SCC090 *HEY1*-OE and control cells (Fig. 1B). By contrast, western blot analysis revealed a decreased E-cadherin expression in all *HEY1*-OE cells. Furthermore, the expression of fibronectin,

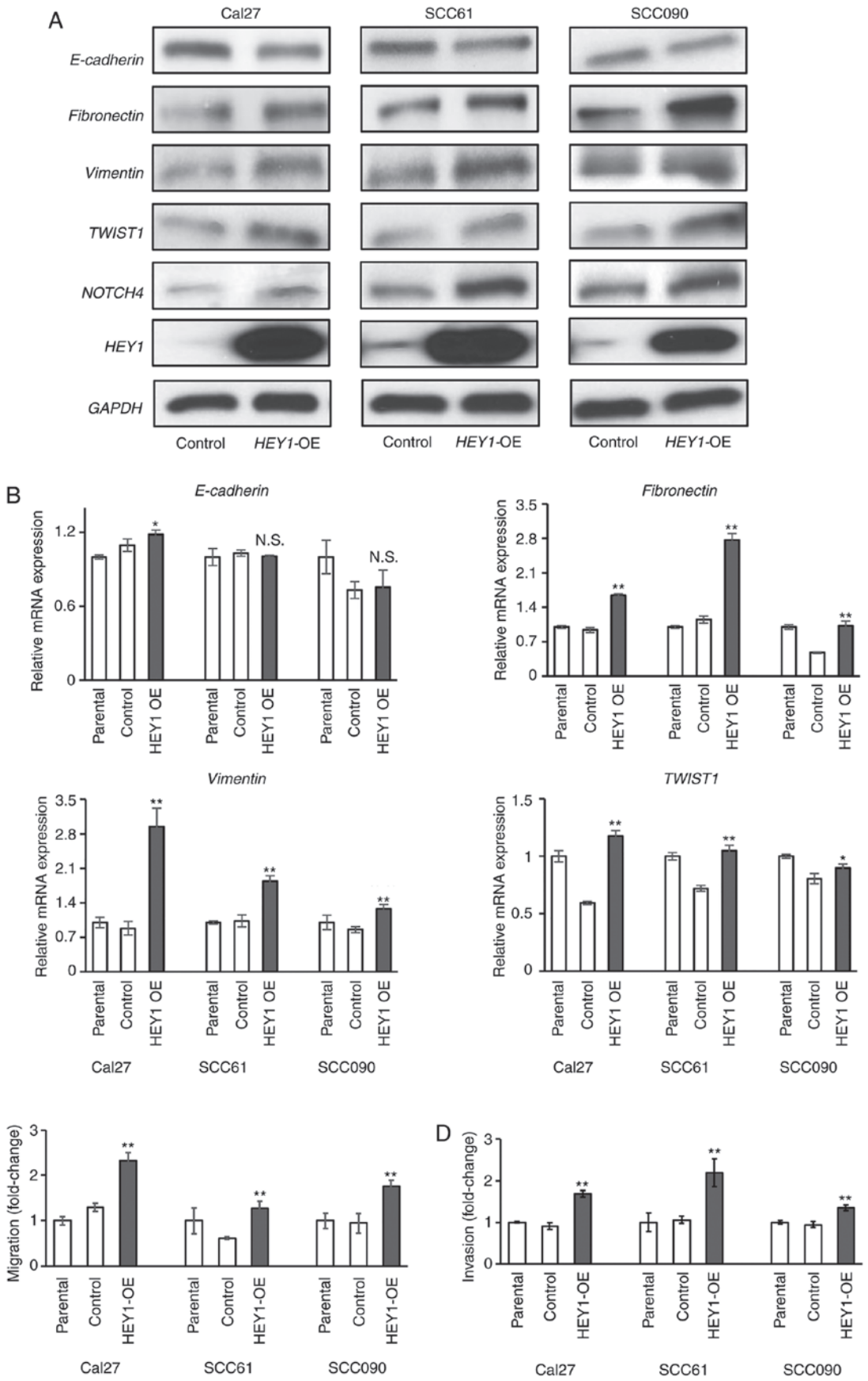

Figure 1. EMT phenotypes in *HEY1*-OE cells. (A) Western blot analysis of EMT-related proteins (E-cadherin, Fibronectin, Vimentin and TWIST1), *NOTCH4* and *HEY1* in control and *HEY1*-OE cells. GAPDH was used as a control. (B) EMT-related gene expression in control and *HEY1*-OE cells was measured by RT-qPCR. The expression differences between control and *HEY1*-OE cells are compared. (C) Migration and (D) invasion assays in control, and *HEY1*-OE cells. The migration and invasion indexes are calculated by dividing the number of control cells through the chamber. The differences between control and *HEY1*-OE cells are compared. P-values were calculated using Dunnett's t-test. *P<0.05, **P<0.01; N.S., not significant. EMT, epithelial-mesenchymal transition; *HEY1*-OE cells, HEY1-overexpressing cells.

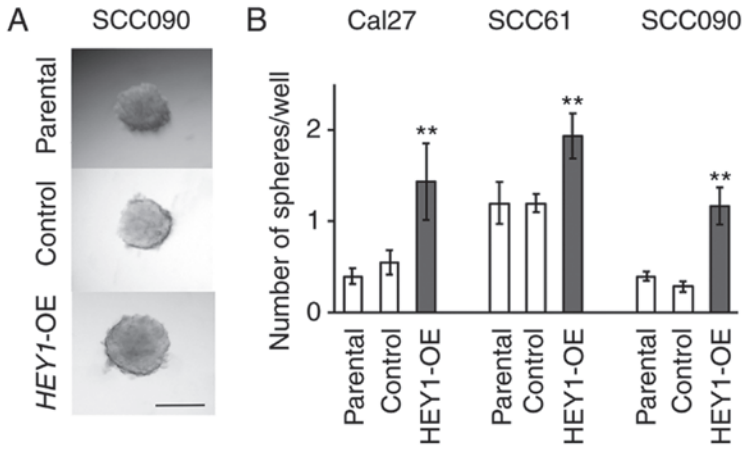

Figure 2. Sphere formation assay in *HEY1*-OE cells. (A) Representative images of sphere colony shapes in SCC090 cells. Scale bar, 100 μm. (B) The number of sphere colonies in each well. The differences between control and *HEY1*-OE cells are compared. P-values were calculated using Dunnett's t-test. **P<0.01. *HEY1*-OE cells, HEY1-overexpressing cells.

Vimentin and TWIST1 increased in all the HNSCC *HEY1*-OE cells (Fig. 1A). EMT is associated with increased cellular migration and invasion; therefore, migration and invasion assays were performed to determine the mechanisms through which the changes in mRNA and protein expression affected the cell phenotype *in vitro*. Increased migration and invasion were noted in the *HEY1*-OE cells compared to the control cells (Figs. 1C and D, and S1B). These results reveal that *HEY1* promotes HNSCC EMT, migration and invasion.

HEY1 promotes sphere formation ability. Spheroids were generated to define the increase in the expression of EMT-related genes associated with sphere formation (25). The present study compared the number of sphere colonies between the *HEY1*-OE and control cells. No evident differences in sphere shape were noted between the control and *HEY1*-OE cells (Fig. 2A); however, the *HEY1*-OE cells formed significantly more spheroids in all cell lines (Fig. 2B). The number of spheroids in the *HEY1*-OE group was several folds higher than that of the control group (Cal27 cells, 2.60; SCC61 cells, 1.61; SCC090 cells, 4.18) (Fig. 2B). These results indicate that *HEY1* promotes spheroid formation.

HEY1 promotes HNSCC tumorigenicity. A proliferation assay was performed to assess phenotypic characteristics affected by *HEY1*. A statistically significant increase in proliferation was observed in all *HEY1*-OE cells compared to the control cells (Fig. S2A). The tumorigenicity of the Cal27 *HEY1*-OE cells was then examined using a nude mouse xenograft model. *HEY1* expression in these tumors was confirmed to be markedly higher in the *HEY1*-OE cell tumors than in the control cell tumors using RT-qPCR and western blot analysis (Fig. 3A). Immunohistochemical staining for HEY1 also revealed that the xenograft tumors generated from *HEY1*-OE cells exhibited a higher HEY1 expression than those from the control cells (Fig. 3B). The *HEY1*-OE cells also generated significantly larger tumors than the control cells (Figs. S2B and 3C), confirmed by an increased tumor weight of the Cal27 *HEY1*-OE tumors compared to the control tumors following tumor excision. The maximum tumor diameter was 12.9 mm in the control group, and 14.9 mm in the *HEY1*-OE group (Fig. 3D).

SOX2 expression correlates with HEY1 expression. Several studies have indicated that *SOX2* is associated with EMT and a CSC state (26-28). In the present study, to elucidate a potential *SOX2* and *HEY1* association in HNSCC, the correlation between *HEY1* and *SOX2* was examined using the TCGA mRNA sequence data from 522 HNSCC and 44 normal tissues samples. A significant positive correlation was noted between *SOX2* and *HEY1* mRNA expression in HNSCC (r=0.45, P<0.0001); however, no significant correlation between these genes was found in the normal tissues (Fig. 4A). Furthermore, other *NOTCH* downstream genes, such as *HES1* and *HES5* did not exhibit any significant positive correlations with *SOX2* (Fig. S3A). Of note, this association was independent of the HPV status (Fig. S3B). To explore this *in vitro*, *SOX2*-overexpressing (*SOX2*-OE) and control cells were generated (Fig. S3C). RT-qPCR demonstrated a significant increase in *HEY1* expression in all HNSCC *SOX2*-OE cells examined. The *SOX2*-OE cells exhibited an approximately 1.5- to 2.0-fold higher *HEY1* expression in all cell lines (Fig. 4B). However, *HES1* expression did not differ significantly between the *SOX2*-OE and control Cal27 and SCC090 cells. The SCC61 *SOX2*-OE cells exhibited a significantly lower *HES1* expression compared to the control cells (Fig. 4C). All *SOX2*-OE cells exhibited a higher HEY1 expression, as shown by western blot analysis. However, HES1 expression between the *SOX2*-OE and control cells did not exhibit a marked difference (Fig. 4D). Among the 3 cell lines, it was found that both SOX2 and HEY1 expression was higher in the Cal27 control cells. This result indicated that there was an association between *SOX2* and *HEY1* expression in HNSCC wild-type cells (Fig. 4D). These results demonstrated that *SOX2* regulated *HEY1* expression in HNSCC.

SOX2 directly binds the HEY1 promoter in HNSCC. To assess whether *SOX2* directly binds *HEY1* promoter region, a luciferase vector with the *HEY1* promoter region was transfected into *SOX2*-OE and control cells. A significant increase in luciferase activity was observed in all HNSCC *SOX2*-OE cells (Fig. 4E). A ChIP qPCR was then performed to validate this result. *SOX2* is a transcription factor that binds to the DNA consensus sequence (T/A)(T/A)CAAAGA (29) or AACAA(A/T)(G/A)(G/A) (30). A candidate *SOX2* binding

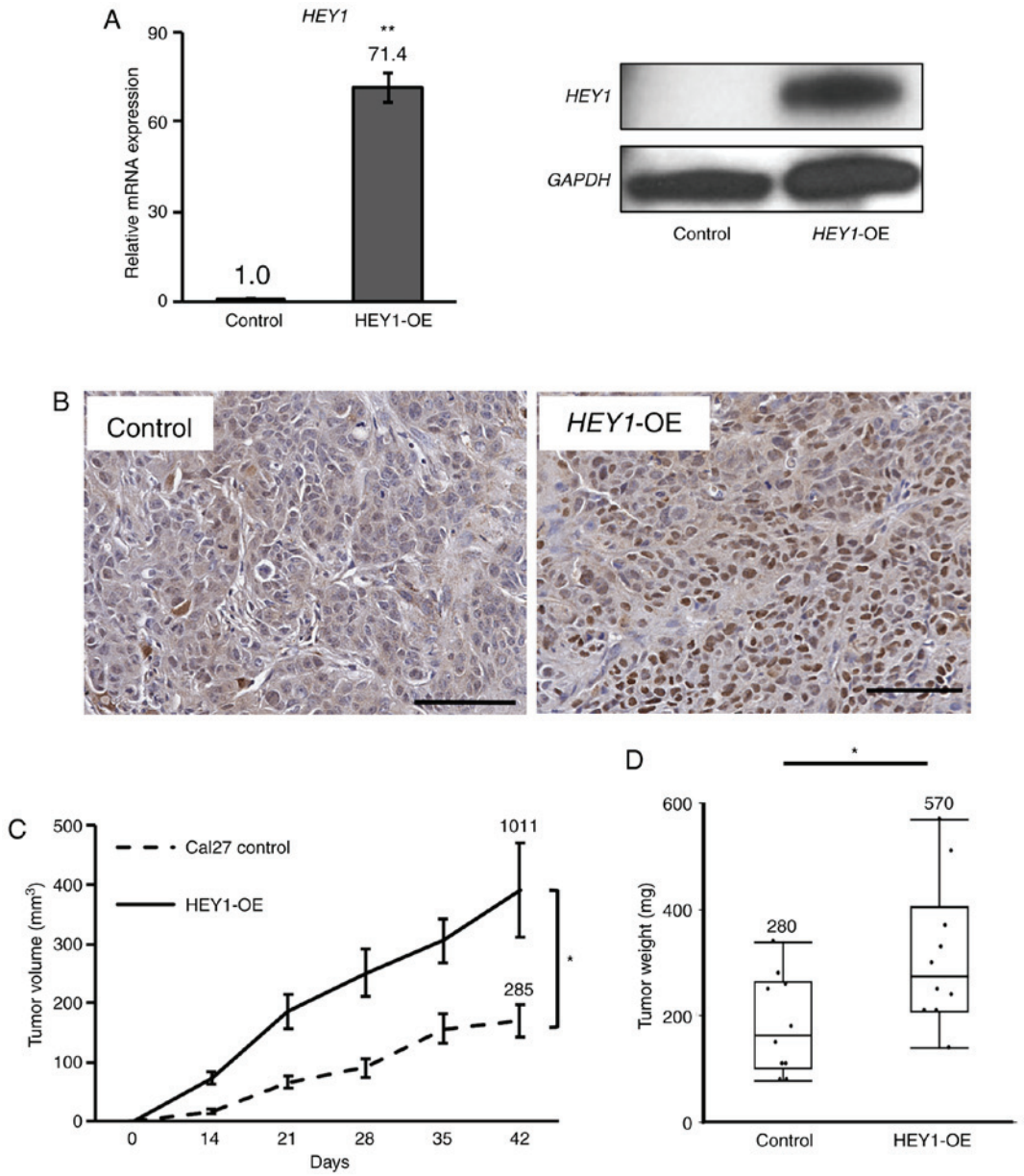

Figure 3. Mouse xenograft tumorigenicity with *HEY1*-OE cells. (A) Analyses for *HEY1* expression in xenograft tumors arising from *HEY1*-OE and control Cal27 cells by RT-qPCR and western blot analysis. A *GAPDH* antibody was used as a control. (B) *HEY1* immunohistochemistry of xenograft tumors arising from control and *HEY1*-OE Cal27 cells. Scale bar, 80 μm. (C) Growth of mouse xenograft tumors. These mice were injected with $2x10^6$ cells of *HEY1*-OE and control Cal27 cells into their flanks. (D) The tumor weight of *HEY1*-OE and control Cal27 cells. Maximum tumor volume and weight are shown on each graph. Whisker plots indicate the minimum and maximum values. P-values were calculated using a Student's t-test. *P<0.05, **P<0.01. *HEY1*-OE cells, HEY1-overexpressing cells.

sequence was found from -1,028 to -1,035 bp upstream of the *HEY1* transcript starting site. Therefore, a ChIP qPCR primer pair was created that bound to this sequence (Fig. 4F). The results of ChIP qPCR revealed that the parental control and stable *SOX2*-OE cells incubated with a *SOX2* antibody exhibited significantly higher enrichment compared to those incubated with IgG antibodies (Fig. 4G). These results demonstrated that *SOX2* can bind and activate the *HEY1* promoter in HNSCC.

SOX2 correlates with HEY1 expression in HNSCC and other SCCs. To examine whether *SOX2* is related to *HEY1* expression in other types of cancer, this association was explored using a TCGA dataset from multiple types of cancers (Table I). SCCs, including HNSCC, esophageal and lung cancer, exhibited a significantly higher *HEY1* expression compared to normal tissues. By contrast, other cancer types, such as lung adenocarcinoma, colon, breast and prostate cancer, exhibited a significantly lower *HEY1* expression compared to normal tissues. All types of SCC exhibited an approximately 1.5- to 1.8-fold higher *HEY1* expression compared to normal cells (Table I). The correlation between *HEY1* and *SOX2* was also compared using the TCGA dataset for each type of cancer. Similar to HNSCC (Fig. 4A and Table I), significant positive correlations were found between *SOX2* and *HEY1 in* esophageal and lung SCC. The *SOX2-HEY1* correlation coefficients in lung adenocarcinoma, colon, breast and prostate were <0.20, indicating a weak correlation (Table I).

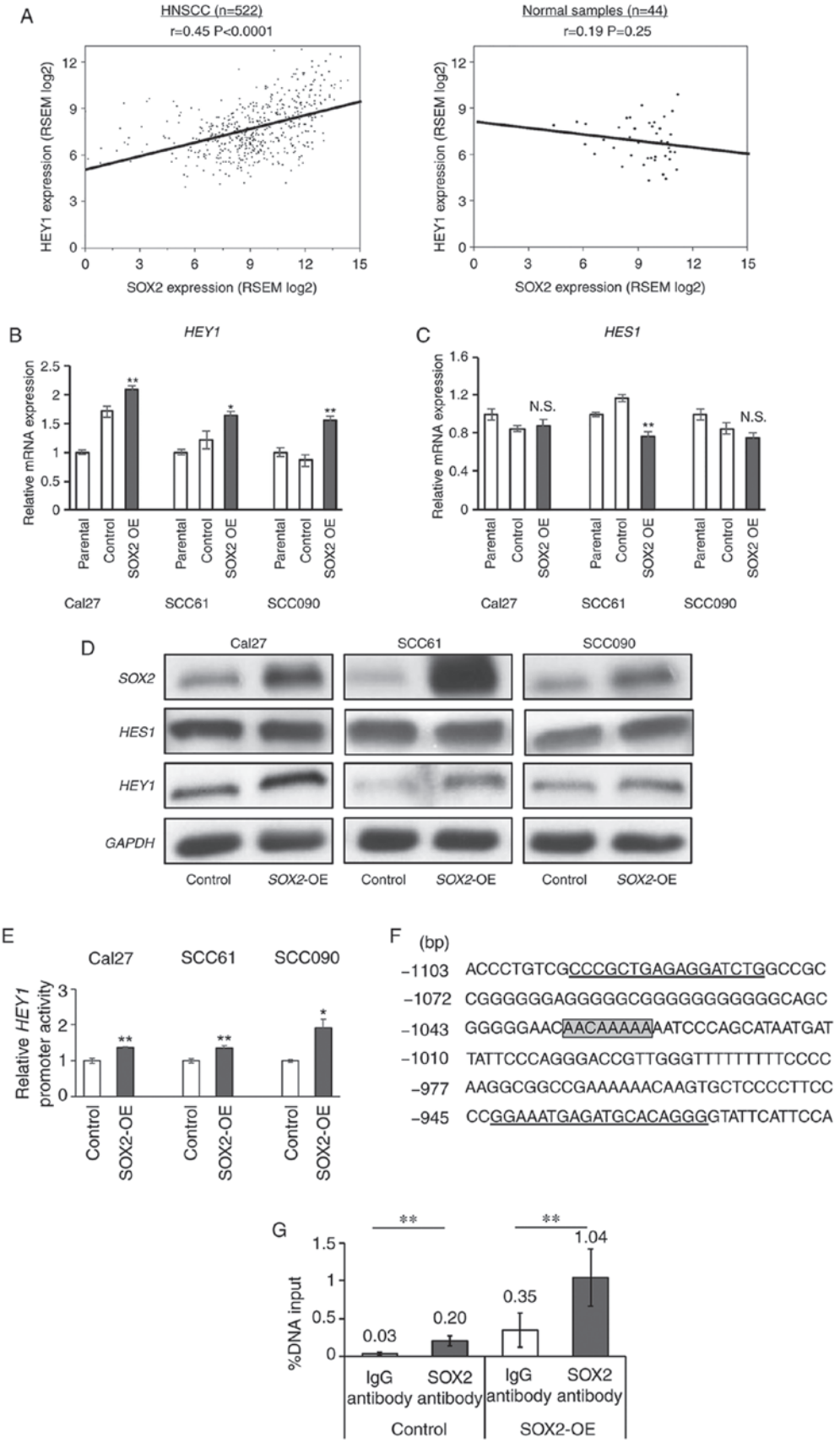

Figure 4. *SOX2* binds the *HEY1* promoter region. (A) The correlations between *SOX2* and *HEY1* were examined using the TCGA HNSCC dataset, including HNSCC (n=522) and normal samples (n=44). 'r' indicates the Pearson's correlation coefficient. (B) *HEY1* and (C) *HES1* expression was compared between *SOX2*-OE and control cells by RT-qPCR. P-values were calculated using Dunnett's t-test. (D) Western blot analysis of *SOX2*, *HES1* and *HEY1* in *SOX2*-OE and control cells. GAPDH is used as a control. (E) Luciferase reporter assays are performed with vectors containing the *HEY1* promoter region. (F) A *SOX2* binding region of the human *HEY1* promoter (shadow box) with primer pairs (underlined). Bp indicates the base pairs from the transcription starting site. (G) ChIP qPCR analysis using the *HEY1* promoter primer in SCC61 *SOX2*-OE and parental control cells. Mouse IgG antibody is used as a negative control. P-values were calculated using a Student's t-test. *P<0.05, **P<0.01; N.S., not significant. *HEY1*-OE cells, HEY1-overexpressing cells.

Table I. TCGA dataset analysis of *HEY1* expression ratios between cancer and normal tissues and *SOX2-HEY1* correlation coefficients in several cancer types.

Cancer types	Number of tumor samples	Number of normal samples	*HEY1* expression ratio (tumor/normal)	P-value	*SOX2-HEY1* correlation coefficient in tumor samples	P-value	*SOX2-HEY1* correlation coefficient in normal samples	P-value
HNSCC	522	44	1.78	<0.0001	0.45	<0.0001	0.18	0.25
Esophageal carcinoma	185	11	1.80	0.082	0.57	<0.0001	-0.56	0.073
Lung SCC	501	51	1.46	0.0003	0.57	<0.0001	0.35	0.011
Lung adenocarcinoma	517	59	0.39	<0.0001	0.12	0.0076	0.024	0.85
Colon adenocarcinoma	459	41	0.58	<0.0001	0.20	0.0001	0.099	0.54
Breast carcinoma	1100	112	0.53	<0.0001	0.15	<0.0001	0.016	0.088
Prostate adenocarcinoma	498	52	0.72	0.011	0.12	0.0088	0.58	<0.0001

HNSCC, head and neck squamous cell carcinoma.

HEY1 correlates with NOTCH4 expression. *HEY1* is a *NOTCH* target gene; however, a previous study by the authors demonstrated a significantly lower *NOTCH4* expression in HNSCC cells in which *HEY1* was knocked down (17). Based on this result, it was hypothesized that *HEY1* also reciprocally increased *NOTCH4* expression directly through the *NOTCH4* promoter. Therefore, the correlation between *NOTCH4* and *NOTCH* downstream genes, including *HEY1*, was examined using the head and neck TCGA dataset (Fig. 5A). A positive correlation was noted between *NOTCH4* and *HEY1* mRNA expression (r=0.39, P<0.0001). However, no significant positive correlation was found between *NOTCH4* and *HES1* and *5* (Fig. 5A). This correlation between *NOTCH4* and *HEY1* was also independent of the HPV status (Fig. S4A). When the association between all *NOTCH* receptors and *HEY1* was compared, *NOTCH4* exhibited the highest positive correlation to *HEY1* of all the *NOTCH* receptors (Figs. S4B and 5A). RT-qPCR revealed a significantly increased *NOTCH4* expression in the Cal27 and SCC61 *HEY1*-OE cells. *NOTCH4* expression did not differ significantly between the SCC090 *HEY1*-OE and control cells (Fig. 5B). All the *HEY1*-OE cells exhibited an elevated NOTCH4 expression, as shown by western blot analysis (Fig. 1A). Therefore, the present study examined whether *HEY1* directly binds the *NOTCH4* promoter region and promotes its transcription, similar to the association of *SOX2* and *HEY1*.

HEY1 directly binds the NOTCH4 promoter in HNSCC. To assess whether *HEY1* directly binds *NOTCH4* promoter region, a luciferase vector with a *NOTCH4* promoter region was transfected into *HEY1*-OE and control cells. A significant increase in luciferase activity was observed in all HNSCC *HEY1*-OE cells (Fig. 5C). The *HEY1* gene binds E-box (CANGTG) and N-box (CACNAG) sites (31,32). Three candidates of *HEY1* binding sequences were found from -884 to -922 bp upstream of the *NOTCH4* transcript starting site. Therefore, a ChIP qPCR primer pair that bound this region was generated (Fig. 5D). The ChIP qPCR results revealed that the parental control and stable *HEY1*-OE cells incubated with a *HEY1* antibody exhibited significantly higher enrichment compared to those incubated with IgG antibodies (Fig. 5E). These data demonstrate that *HEY1* can bind the *NOTCH4* promoter in HNSCC and drive *NOTCH4* expression.

The associations between these genes are summarized in Fig. 6; these data demonstrate that *SOX2* regulates *HEY1* and *HEY1* creates a reciprocal loop with *NOTCH4* to promote HNSCC EMT, sphere formation and tumorigenicity.

Discussion

Previous studies have revealed that the *NOTCH* pathway is upregulated in HNSCC and that *NOTCH* expression is related to an advanced clinical stage (33,34). In a previous study, the authors observed a specific upregulation of the *NOTCH4-HEY1* pathway in HNSCC (17). In the present study, further analysis of a specific *NOTCH* pathway and a new mechanism of functional integration is reported between *SOX2* and the *NOTCH4-HEY1* axis.

It was found that the *HEY1-OE* cells increased proliferation and tumorigenicity in xenograft models. *HEY1*-OE cells

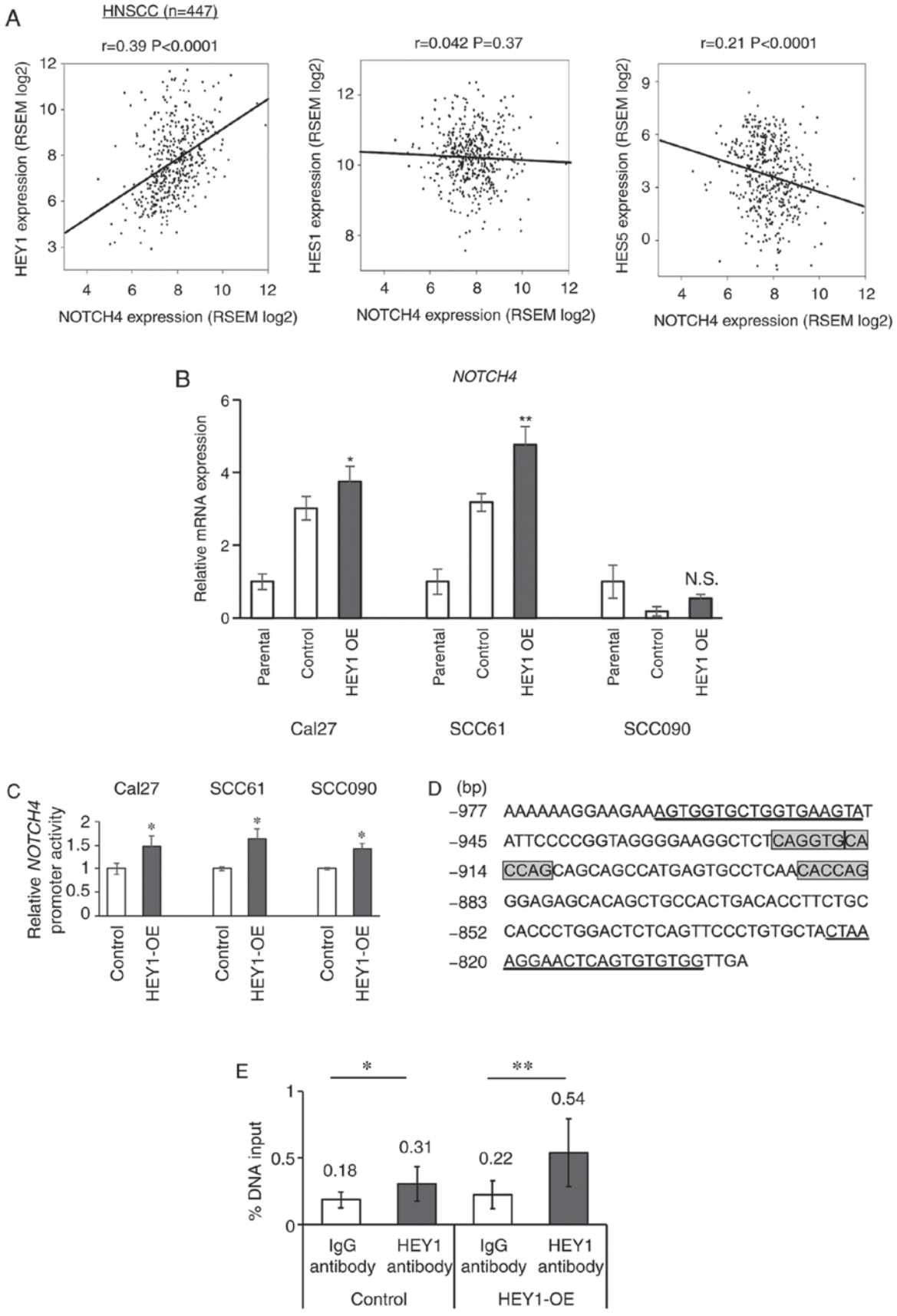

Figure 5. *HEY1* binds the *NOTCH4* promoter region. (A) The correlations between *NOTCH4* and *NOTCH* downstream genes were examined using the TCGA HNSCC dataset, including *NOTCH* wild-type HNSCC (n=447). HNSCC samples with *NOTCH* mutations are excluded (n=73). 'r' indicates the Pearson's correlation coefficient. (B) *NOTCH4* expression was compared between *HEY1*-OE and control cells by RT-qPCR. P-values were calculated using Dunnett's t-test. (C) Luciferase reporter assay performed with vectors containing the *NOTCH4* promoter region. (D) *HEY1* binding regions of the human *NOTCH4* promoter (shadow box) with primer pairs (underlined). Bp indicates the base pairs from the transcription starting site. (E) ChIP qPCR analysis using the *NOTCH4* promoter primer in SCC61 *SOX2*-OE and parental control cells. Mouse IgG antibody is used as a negative control. *P<0.05, **P<0.01; N.S., not significant. *HEY1*-OE cells, HEY1-overexpressing cells.

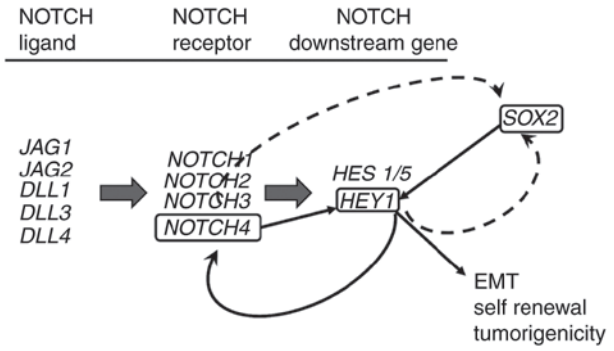

Figure 6. The scheme of the present study. *SOX2* regulates *HEY1* and *HEY1* creates a reciprocal loop with *NOTCH4* to promote HNSCC EMT, self renewal and tumorigenicity.

also increased cell invasion and migration, known as EMT ability, and promoted sphere formation, reflecting a phenotype of cell stemness, self-renewal ability *in vitro* (35-37). As shown in Fig. 1B, *E-cadherin* expression was higher in the Cal27 *HEY1*-OE than the control cells, and did not differ significantly between the *HEY1*-OE and control SCC61 and SCC090 cells. By contrast, western blot analysis revealed a decreased E-cadherin expression in all *HEY1*-OE cells (Fig. 1A). This may be due to post-translational processing, as the post-translational *E-cadherin* modification is known to induce EMT in cancer (38). *E-cadherin* mRNA and protein expression differed in all *HEY1-OE* cells. Furthermore, the expression levels of mesenchymal genes, such as *fibronectin, Vimentin* and *TWIST1* in the *HEY1*-OE cells were increased in all HNSCC cells (Fig. 1B). Western blot analysis of N-cadherin expression was also performed in these cells; however, no increase in N-cadherin increase expression was found in the *HEY1*-OE cells (Fig. S4C). The reason for this lack of change in N-cadherin expression is not clear. The present study did not validate N-cadherin and E-cadherin expression in control and *HEY1-OE* cells using immunocytochemistry. This is a limitation of the present study. However, the authors have previously demonstrated that *N-cadherin* expression was significantly increased in the *HEY1* high expression group in HNSCC patients using a TCGA dataset (17). Thus, these *in vitro* assay results demonstrated that *HEY1* promotes EMT in HNSCC.

HEY1 expression significantly correlated with *SOX2* expression in the TCGA dataset and in *in vitro* experiments. *SOX2* is an EMT inducer gene that promotes HNSCC cell invasion and migration (23,28,39). *SOX2* and *HEY1* are early sensory markers that exist in the same domain in mice inner ear development (40) and *SOX2* is co-expressed with *HEY1*/*HEY2* in the inner ear (41). In glioma CSC, both *SOX2* and *HEY1* expression is increased compared to non-CSC glioma cells (42). Chen *et al* demonstrated that *JAG1* promoted *HEY1* and *SOX2* expression, and *NOTCH* inhibition by a gamma secretase inhibitor decreased *SOX2* promoter activity in breast cancer cells (43). However, these studies did not examine which *NOTCH* related genes directly interacted with the *SOX2* promoter (43). In this context, the present study examined the association between *SOX2* and *HEY1*. As noted above, the reporter and ChIP assays indicated that *SOX2* regulated *HEY1* expression via binding to its promoter. There are no commercially available *SOX2* blocking antibodies. Thus, the authors were not able to define *HEY1* expression and an EMT phenotype using *SOX2* blocking antibody. Of note, the present study did not perform *SOX2* mutational analysis in reporter assays of *HEY1* that would allow the precise localization of the *SOX2* binding *HEY1* promoter within a 1-2 kb segment. The authors have previously demonstrated that *HEY1* expression was significantly increased in sphere cells of HNSCC cell lines; *HEY1* expression in sphere cells was increased approximately 1.4- to 3.5-fold compared with parental cells (17). In the present study, it was demonstrated that *HEY1* promotes sphere formation and tumorigenicity that are closely related to a cancer stem cell phenotype. These results indicate that *SOX2* maintains HNSCC CSCs through *HEY1* expression.

A previous study by the authors demonstrated that *HEY1* knockdown HNSCC cells decreased *SOX2* expression, as shown by RT-qPCR and western blot analysis (17). These two results indicate that *SOX2* and *HEY1* may exist in a reciprocal loop similar to that of *NOTCH4-HEY1*. On the other hand, Wang *et al* demonstrated that glioma stem cells made a *NOTCH1-SOX2* positive feedback loop (44). The TCGA analysis in the previous study by the authors also indicated that *NOTCH4* and *SOX2* expression had a significant positive correlation (17). These results indicate that *NOTCH4* may promote *SOX2* expression in HNSCC similar to *HEY1* expression (Fig. 6). If *NOTCH4* promotes *SOX2* expression, this may explain why cells in which *HEY1* was knocked down had a decreased *SOX2* expression, as *HEY1* knockdown in cells decreased *NOTCH4* expression (Fig. 6). Previous studies have indicated this connection in neural stem cells and brain endothelial cells; *NOTCH* increases *SOX2* promoter activity and regulates *SOX2* expression (45,46).

Furthermore, the current TCGA dataset analysis also revealed that *SOX2* correlates with *HEY1* expression in several SCCs, but not in non-SCC cancers or normal tissue (Table I). There are several studies on *SOX2* function in SCC and its promotion of tumorigenesis, metastasis and EMT (21,47,48). As regards *HEY1* function in SCC, Forghanifard *et al* examined *NOTCH* pathway gene expression in 50 patients with esophageal SCC and indicated that *HEY1* and *HEY2* expression were significantly associated with clinical stage and a poor prognosis (49). The results of the present study and these reports indicate that *HEY1* upregulation promotes tumor progression, and that a *SOX2-HEY1* expression correlation is found predominantly in SCC, reinforcing a context dependent setting for activation of the *NOTCH4-HEY1* pathway. However, the TCGA dataset shows only each mRNA expression of individual patients. The present study performed a functional analysis for these molecules in HNSCC, but not in other SCC types, limiting functional confirmation in these systems.

In the present study, the reporter and ChIP assays also indicated that *HEY1* reciprocally regulated *NOTCH4* expression via binding to its promoter. James *et al* demonstrated that the *NOTCH4* was ligand unresponsive in *NOTCH* signaling (50). These results may explain why the *NOTCH4-HEY1* pathway was specifically upregulated in HNSCC. Of note, specific mutational analysis in *NOTCH4* reporter assays to precisely

localize the *HEY1* binding site would add further depth to the current understanding of this interaction. Nevertheless, the results of additional mutational analysis would not substantively alter the conclusions based on these data, that *SOX2* and *HEY1* interact with these promoter regions. The present study did not explore the ability of specific *NOTCH* ligands, such as *JAG1, JAG2, DLL1, DLL3* and *DLL4* in the activation of the *NOTCH4-HEY1* pathway, which is a limitation of the present study, as this may provide further data that support the model of constitutive activation in the absence of exogenous ligand. The present study did not assess whether *HEY1* bound to the *NOTCH1-3* promoter, and *NOTCH1* and *2* expression was lower in HNSCC than normal samples; however, *NOTCH3* expression was slightly higher in HNSCC than normal tissue, which is similar to *NOTCH4* (51). *NOTCH3* also significantly and positively correlated with *HEY1* expression. *NOTCH4* was more significantly and highly expressed in HNSCC and positively correlated with *HEY1* than *NOTCH3* (Figs. 4A and S4B) (51). Notably, a similar correlation was found between *NOTCH4* and *HEY1, HES1* and *HES5* in head and neck normal samples of the TCGA dataset and HNSCC (Figs. 5A and S4D). A moderately positive correlation was noted only between *NOTCH4* and *HEY1* mRNA expression in normal samples (r=0.52, P=0.0003). It was hypothesized that the *NOTCH4*/*HEY1* pathway is a specific pathway not only active in HNSCC, but potentially active in head and neck normal epithelial cells. Based on these findings, previous studies have reported trials of anti-*NOTCH* therapy for HNSCC (52,53).

In conclusion, the present study demonstrates that *HEY1* expression in HNSCC is regulated by *SOX2* and promotes EMT. The *NOTCH4*/*HEY1*/*SOX2* pathway is specifically upregulated and creates a positive reciprocal loop in HNSCC, defining a pathway that may be a novel target for HNSCC therapy.

Acknowledgements

Not applicable.

Funding

The National Institute of Dental and Craniofacial Research (NIDCR no. R01DE023347) supported the present study. JAC received this grant. Apart from for this grant, no potential conflicts of interest are disclosed.

Availability of data and materials

The datasets used and/or analyzed during the current study are available from the corresponding author on reasonable request.

Authors' contributions

The study was designed and conceived by TF, TWG and JAC. The experimental procedures and data analysis were carried out by TF, SR, MA and JAC. The acquisition of data was carried out by TF, SH, CL, AS, YS and SS. The manuscript was prepared by TF and JAC. All authors read and approved the final manuscript.

Ethics approval and consent to participate

All mice were handled in accordance with the procedures outlined in the Regulations on Animal Experiments at University of California San Diego. The Institution Animal Care and Use Committee in University of California San Diego approved the study.

Patient consent for publication

Not applicable.

Competing interests

The authors declare that they have no competing interests.

References

1. Leemans CR, Braakhuis BJ and Brakenhoff RH: The molecular biology of head and neck cancer. Nat Rev Cancer 11: 9-22, 2011.
2. Pignon JP, le Maître A, Maillard E, Bourhis J; MACH-NC Collaborative Group: Meta-analysis of chemotherapy in head and neck cancer (MACH-NC): An update on 93 randomised trials and 17,346 patients. Radiother Oncol 92: 4-14, 2009.
3. Bernier J, Domenge C, Ozsahin M, Matuszewska K, Lefèbvre JL, Greiner RH, Giralt J, Maingon P, Rolland F, Bolla M, *et al*: Postoperative irradiation with or without concomitant chemotherapy for locally advanced head and neck cancer. N Engl J Med 350: 1945-1952, 2004.
4. Cooper JS, Pajak TF, Forastiere AA, Jacobs J, Campbell BH, Saxman SB, Kish JA, Kim HE, Cmelak AJ, Rotman M, *et al*: Postoperative concurrent radiotherapy and chemotherapy for high-risk squamous-cell carcinoma of the head and neck. N Engl J Med 350: 1937-1944, 2004.
5. Agrawal N, Frederick MJ, Pickering CR, Bettegowda C, Chang K, Li RJ, Fakhry C, Xie TX, Zhang J, Wang J, *et al*: Exome sequencing of head and neck squamous cell carcinoma reveals inactivating mutations in NOTCH1. Science 333: 1154-1157, 2011.
6. Stransky N, Egloff AM, Tward AD, Kostic AD, Cibulskis K, Sivachenko A, Kryukov GV, Lawrence MS, Sougnez C, McKenna A, *et al*: The mutational landscape of head and neck squamous cell carcinoma. Science 333: 1157-1160, 2011.
7. Sun W, Gaykalova DA, Ochs MF, Mambo E, Arnaoutakis D, Liu Y, Loyo M, Agrawal N, Howard J, Li R, *et al*: Activation of the NOTCH pathway in head and neck cancer. Cancer Res 74: 1091-1104, 2014.
8. Kalaitzidis D and Armstrong SA: Cancer: The flipside of Notch. Nature 473: 159-160, 2011.
9. Sethi N, Dai X, Winter CG and Kang Y: Tumor-derived JAGGED1 promotes osteolytic bone metastasis of breast cancer by engaging notch signaling in bone cells. Cancer Cell 19: 192-205, 2011.
10. Zavadil J, Cermak L, Soto-Nieves N and Bottinger EP: Integration of TGF-beta/Smad and Jagged1/Notch signalling in epithelial-to-mesenchymal transition. EMBO J 23: 1155-1165, 2004.
11. Fischer A, Steidl C, Wagner TU, Lang E, Jakob PM, Friedl P, Knobeloch KP and Gessler M: Combined loss of Hey1 and HeyL causes congenital heart defects because of impaired epithelial to mesenchymal transition. Circ Res 100: 856-863, 2007.
12. Luna-Zurita L, Prados B, Grego-Bessa J, Luxán G, del Monte G, Benguría A, Adams RH, Pérez-Pomares JM and de la Pompa JL: Integration of a Notch-dependent mesenchymal gene program and Bmp2-driven cell invasiveness regulates murine cardiac valve formation. J Clin Invest 120: 3493-3507, 2010.
13. Tsung AJ, Guda MR, Asuthkar S, Labak CM, Purvis IJ, Lu Y, Jain N, Bach SE, Prasad DVR and Velpula KK: Methylation regulates HEY1 expression in glioblastoma. Oncotarget 8: 44398-44409, 2017.
14. Shibata S, Marushima H, Asakura T, Matsuura T, Eda H, Aoki K, Matsudaira H, Ueda K and Ohkawa K: Three-dimensional culture using a radial flow bioreactor induces matrix metalloprotease 7-mediated EMT-like process in tumor cells via TGFbeta1/Smad pathway. Int J Oncol 34: 1433-1448, 2009.

15. Man CH, Wei-Man Lun S, Wai-Ying Hui J, To KF, Choy KW, Wing-Hung Chan A, Chow C, Tin-Yun Chung G, Tsao SW, Tak-Chun Yip T, *et al*: Inhibition of NOTCH3 signalling significantly enhances sensitivity to cisplatin in EBV-associated nasopharyngeal carcinoma. J Pathol 226: 471-481, 2012.
16. Rettig EM, Bishop JA, Agrawal N, Chung CH, Sharma R, Zamuner F, Li RJ, Koch WM, Califano JA, Guo T, *et al*: HEY1 is expressed independent of NOTCH1 and is associated with poor prognosis in head and neck squamous cell carcinoma. Oral Oncol 82: 168-175, 2018.
17. Fukusumi T, Guo TW, Sakai A, Ando M, Ren S, Haft S, Liu C, Amornphimoltham P, Gutkind JS and Califano JA: The NOTCH4-HEY1 pathway induces epithelial-mesenchymal transition in head and neck squamous cell carcinoma. Clin Cancer Res 24: 619-633, 2018.
18. Fukusumi T, Ishii H, Konno M, Yasui T, Nakahara S, Takenaka Y, Yamamoto Y, Nishikawa S, Kano Y, Ogawa H, *et al*: CD10 as a novel marker of therapeutic resistance and cancer stem cells in head and neck squamous cell carcinoma. Br J Cancer 111: 506-514, 2014.
19. Prince ME, Sivanandan R, Kaczorowski A, Wolf GT, Kaplan MJ, Dalerba P, Weissman IL, Clarke MF and Ailles LE: Identification of a subpopulation of cells with cancer stem cell properties in head and neck squamous cell carcinoma. Proc Natl Acad Sci USA 104: 973-978, 2007.
20. Chen YC, Chen YW, Hsu HS, Tseng LM, Huang PI, Lu KH, Chen DT, Tai LK, Yung MC, Chang SC, *et al*: Aldehyde dehydrogenase 1 is a putative marker for cancer stem cells in head and neck squamous cancer. Biochem Biophys Res Commun 385: 307-313, 2009.
21. Lee SH, Oh SY, Do SI, Lee HJ, Kang HJ, Rho YS, Bae WJ and Lim YC: SOX2 regulates self-renewal and tumorigenicity of stem-like cells of head and neck squamous cell carcinoma. Br J Cancer 111: 2122-2130, 2014.
22. Du L, Yang Y, Xiao X, Wang C, Zhang X, Wang L, Zhang X, Li W, Zheng G, Wang S and Dong Z: Sox2 nuclear expression is closely associated with poor prognosis in patients with histologically node-negative oral tongue squamous cell carcinoma. Oral Oncol 47: 709-713, 2011.
23. Yang N, Hui L, Wang Y, Yang H and Jiang X: Overexpression of SOX2 promotes migration, invasion, and epithelial-mesenchymal transition through the Wnt/β-catenin pathway in laryngeal cancer Hep-2 cells. Tumour Biol 35: 7965-7973, 2014.
24. Livak KJ and Schmittgen TD: Analysis of relative gene expression data using real-time quantitative PCR and the 2(-Delta Delta C(T)) method. Methods 25: 402-408, 2001.
25. Han XY, Wei B, Fang JF, Zhang S, Zhang FC, Zhang HB, Lan TY, Lu HQ and Wei HB: Epithelial-mesenchymal transition associates with maintenance of stemness in spheroid-derived stem-like colon cancer cells. PLoS One 8: e73341, 2013.
26. Gangemi RM, Griffero F, Marubbi D, Perera M, Capra MC, Malatesta P, Ravetti GL, Zona GL, Daga A and Corte G: SOX2 silencing in glioblastoma tumor-initiating cells causes stop of proliferation and loss of tumorigenicity. Stem Cells 27: 40-48, 2009.
27. Han X, Fang X, Lou X, Hua D, Ding W, Foltz G, Hood L, Yuan Y and Lin B: Silencing SOX2 induced mesenchymal-epithelial transition and its expression predicts liver and lymph node metastasis of CRC patients. PLoS One 7: e41335, 2012.
28. Boumahdi S, Driessens G, Lapouge G, Rorive S, Nassar D, Le Mercier M, Delatte B, Caauwe A, Lenglez S, Nkusi E, *et al*: SOX2 controls tumour initiation and cancer stem-cell functions in squamous-cell carcinoma. Nature 511: 246-250, 2014.
29. Seo E, Basu-Roy U, Zavadil J, Basilico C and Mansukhani A: Distinct functions of Sox2 control self-renewal and differentiation in the osteoblast lineage. Mol Cell Biol 31: 4593-4608, 2011.
30. Salmon-Divon M, Dvinge H, Tammoja K and Bertone P: PeakAnalyzer: Genome-wide annotation of chromatin binding and modification loci. BMC Bioinformatics 11: 415, 2010.
31. Leal MC, Surace EI, Holgado MP, Ferrari CC, Tarelli R, Pitossi F, Wisniewski T, Castano EM and Morelli L: Notch signaling proteins HES-1 and Hey-1 bind to insulin degrading enzyme (IDE) proximal promoter and repress its transcription and activity: Implications for cellular Aβ metabolism. Biochim Biophys Acta 1823: 227-235, 2012.
32. Iso T, Sartorelli V, Poizat C, Iezzi S, Wu HY, Chung G, Kedes L and Hamamori Y: HERP, a novel heterodimer partner of HES/E(spl) in Notch signaling. Mol Cell Biol 21: 6080-6089, 2001.
33. Joo YH, Jung CK, Kim MS and Sun DI: Relationship between vascular endothelial growth factor and Notch1 expression and lymphatic metastasis in tongue cancer. Otolaryngol Head Neck Surg 140: 512-518, 2009.
34. Zhang TH, Liu HC, Zhu LJ, Chu M, Liang YJ, Liang LZ and Liao GQ: Activation of Notch signaling in human tongue carcinoma. J Oral Pathol Med 40: 37-45, 2011.
35. Lim YC, Oh SY, Cha YY, Kim SH, Jin X and Kim H: Cancer stem cell traits in squamospheres derived from primary head and neck squamous cell carcinomas. Oral Oncol 47: 83-91, 2011.
36. Kang Y and Massagué J: Epithelial-mesenchymal transitions: Twist in development and metastasis. Cell 118: 277-279, 2004.
37. Brabletz T, Kalluri R, Nieto MA and Weinberg RA: EMT in cancer. Nat Rev Cancer 18: 128-134, 2018.
38. Shao K, Chen ZY, Gautam S, Deng NH, Zhou Y and Wu XZ: Posttranslational modification of E-cadherin by core fucosylation regulates Src activation and induces epithelial-mesenchymal transition-like process in lung cancer cells. Glycobiology 26: 142-154, 2016.
39. Vanner RJ, Remke M, Gallo M, Selvadurai HJ, Coutinho F, Lee L, Kushida M, Head R, Morrissy S, Zhu X, *et al*: Quiescent sox2(+) cells drive hierarchical growth and relapse in sonic hedgehog subgroup medulloblastoma. Cancer Cell 26: 33-47, 2014.
40. Pan W, Jin Y, Stanger B and Kiernan AE: Notch signaling is required for the generation of hair cells and supporting cells in the mammalian inner ear. Proc Natl Acad Sci USA 107: 15798-15803, 2010.
41. Benito-Gonzalez A and Doetzlhofer A: Hey1 and Hey2 control the spatial and temporal pattern of mammalian auditory hair cell differentiation downstream of Hedgehog signaling. J Neurosci 34: 12865-12876, 2014.
42. Fang KM, Lin TC, Chan TC, Ma SZ, Tzou BC, Chang WR, Liu JJ, Chiou SH, Yang CS and Tzeng SF: Enhanced cell growth and tumorigenicity of rat glioma cells by stable expression of human CD133 through multiple molecular actions. Glia 61: 1402-1417, 2013.
43. Chen JY, Li CF, Chu PY, Lai YS, Chen CH, Jiang SS, Hou MF and Hung WC: Lysine demethylase 2A promotes stemness and angiogenesis of breast cancer by upregulating Jagged1. Oncotarget 7: 27689-27710, 2016.
44. Wang J, Xu SL, Duan JJ, Yi L, Guo YF, Shi Y, Li L, Yang ZY, Liao XM, Cai J, *et al*: Invasion of white matter tracts by glioma stem cells is regulated by a NOTCH1-SOX2 positive-feedback loop. Nat Neurosci 22: 91-105, 2019.
45. Ehm O, Göritz C, Covic M, Schäffner I, Schwarz TJ, Karaca E, Kempkes B, Kremmer E, Pfrieger FW, Espinosa L, *et al*: RBPJkappa-dependent signaling is essential for long-term maintenance of neural stem cells in the adult hippocampus. J Neurosci 30: 13794-13807, 2010.
46. Wu X, Yao J, Wang L, Zhang D, Zhang L, Reynolds EX, Yu T, Bostrom KI and Yao Y: Crosstalk between BMP and Notch induces Sox2 in cerebral endothelial cells. Cells 8: 549, 2019.
47. Ferone G, Song JY, Sutherland KD, Bhaskaran R, Monkhorst K, Lambooij JP, Proost N, Gargiulo G and Berns A: SOX2 is the determining oncogenic switch in promoting lung squamous cell carcinoma from different cells of origin. Cancer Cell 30: 519-532, 2016.
48. Bochen F, Adisurya H, Wemmert S, Lerner C, Greiner M, Zimmermann R, Hasenfus A, Wagner M, Smola S, Pfuhl T, *et al*: Effect of 3q oncogenes SEC62 and SOX2 on lymphatic metastasis and clinical outcome of head and neck squamous cell carcinomas. Oncotarget 8: 4922-4934, 2017.
49. Forghanifard MM, Taleb S and Abbaszadegan MR: Notch signaling target genes are directly correlated to esophageal squamous cell carcinoma tumorigenesis. Pathol Oncol Res 21: 463-467, 2015.
50. James AC, Szot JO, Iyer K, Major JA, Pursglove SE, Chapman G and Dunwoodie SL: Notch4 reveals a novel mechanism regulating Notch signal transduction. Biochim Biophys Acta 1843: 1272-1284, 2014.
51. Fukusumi T and Califano JA: The NOTCH pathway in head and neck squamous cell carcinoma. J Dent Res 97: 645-65, 2018.
52. Yu S, Zhang R, Liu F, Hu H, Yu S and Wang H: Down-regulation of Notch signaling by a γ-secretase inhibitor enhances the radiosensitivity of nasopharyngeal carcinoma cells. Oncol Rep 26: 1323-1328, 2011.
53. Zhao ZL, Zhang L, Huang CF, Ma SR, Bu LL, Liu JF, Yu GT, Liu B, Gutkind JS, Kulkarni AB, *et al*: NOTCH1 inhibition enhances the efficacy of conventional chemotherapeutic agents by targeting head neck cancer stem cell. Sci Rep 6: 24704, 2016.